Regulation of Flagellar Dynein by Phosphorylation of a 138-kD Inner Arm Dynein Intermediate Chain

Geoffrey Habermacher and Winfield S. Sale

Department of Anatomy and Cell Biology, Emory University School of Medicine, Atlanta, Georgia 30322

Abstract. One of the challenges in understanding ciliary and flagellar motility is determining the mechanisms that locally regulate dynein-driven microtubule sliding. Our recent studies demonstrated that microtubule sliding, in *Chlamydomonas* flagella, is regulated by phosphorylation. However, the regulatory proteins remain unknown. Here we identify the 138-kD intermediate chain of inner arm dynein I1 as the critical phosphoprotein required for regulation of motility. This conclusion is founded on the results of three different experimental approaches. First, genetic analysis and functional assays revealed that regulation of microtubule sliding, by phosphorylation, requires inner arm dynein I1. Second, in vitro phosphorylation indicated the 138-kD intermediate chain of I1 is the only phosphorylated subunit. Third, in vitro reconstitution demonstrated that phosphorylation and dephosphorylation of the 138-kD intermediate chain inhibits and restores wild-type microtubule sliding, respectively. We conclude that change in phosphorylation of the 138-kD intermediate chain of I1 regulates dynein-driven microtubule sliding. Moreover, based on these and other data, we predict that regulation of I1 activity is involved in modulation of flagellar waveform.

Analysis of *Chlamydomonas* flagella has demonstrated that one of the functions of the flagellar central pair/radial spoke apparatus is to control flagellar waveform, and the mechanism involves regulation of flagellar dynein activity (Smith and Sale, 1994; Habermacher and Sale, 1995; Porter, 1996). Flagellar mutants with defective radial spokes or central pair structures are generally paralyzed (Huang, 1986; Curry and Rosenbaum, 1993). However, flagellar paralysis, resulting from defects in the radial spokes or central pair, can be reversed by bypass suppressor mutations that restore motility without repair of the original radial spoke defect (Huang et al., 1982; Porter et al., 1992). Analysis of flagellar motility in suppressed cells demonstrated the radial spokes operate to control the curvature of flagellar bending (Brokaw et al., 1982). Furthermore, the compensating suppressor mutations were found to alter either the dynein arms or a collection of proteins referred to as the dynein regulatory complex (drc)[1] (Huang et al., 1982; Piperno et al., 1992, 1994; Porter et al., 1992; Gardner et al., 1994). Based on these data, it was hypothesized that the radial spokes and the drc regulate flagellar dynein activity (Huang et al., 1982; Porter et al., 1992; Smith and Sale, 1992*a*, 1994). Consistent with this interpretation is the localization of drc components at the junction between the radial spokes and the inner dynein arms (Gardner et al., 1994; Piperno et al., 1994). However, the molecular mechanisms by which the radial spokes and drc serve to control flagellar dynein activity are unclear.

To directly address the hypothesis that radial spokes regulate flagellar dynein activity, the velocity of dynein-driven microtubule sliding was measured in mutant axonemes lacking radial spokes. Smith and Sale (1992*a*) discovered that microtubule sliding is greatly reduced in axonemes missing the radial spokes. Furthermore, in vitro reconstitution experiments demonstrated that the radial spokes are required for wild-type dynein-driven microtubule sliding. Moreover, radial spoke–induced change in microtubule sliding is mediated by posttranslational modification of the inner dynein arms (Smith and Sale, 1992*a*).

Based on studies by Hasegawa et al. (1987), we postulated phosphorylation regulates flagellar dynein activity. Consistent with this hypothesis, protein kinase inhibitors including the peptide inhibitor PKI (selective for cAMP-dependent kinase) and type II regulatory subunit (regulatory subunit of the cAMP-dependent kinase) were found to restore wild-type microtubule sliding in isolated axonemes lacking radial spokes (Howard et al., 1994). In vitro reconstitution experiments, using double mutants missing both outer arm dynein and radial spokes, indicated that one of the target phosphoproteins is located in the inner arm dynein fraction (Howard et al., 1994). We concluded the axoneme contains a cAMP-dependent ki-

Address all correspondence to Winfield S. Sale, Department of Anatomy and Cell Biology, Emory University School of Medicine, Atlanta, GA 30322. Tel.: (404) 727-6265. Fax: (404) 727-6256. e-mail: win@anatomy.emory.edu

1. *Abbreviation used in this paper*: drc, dynein regulatory complex.

nase, presumably associated with inner arm dynein, that inhibits dynein-driven microtubule sliding in paralyzed axonemes. From these results, we predicted increased microtubule sliding also requires the activity of an endogenous phosphatase, also presumed to be in close association with the inner dynein arms. As predicted, restoration of wild-type inner arm dynein activity requires an axonemal type-1 phosphatase, indicating inner arm dynein's microtubule sliding activity is regulated by change in phosphorylation of a key inner arm protein (Habermacher and Sale, 1996). Together the data support a model in which the radial spokes, in conjunction with an axonemal cAMP-dependent kinase and type-1 phosphatase, regulate inner arm dynein activity (see Fig. 1). Our goal was to identify the critical inner arm dynein component.

Structural and biochemical analyses of wild-type and mutant axonemes have established that the inner arm dyneins are heterogeneous in composition and location along each doublet microtubule (Goodenough and Heuser, 1984; Goodenough et al., 1987; Piperno et al., 1990; Piperno and Ramanis, 1991; Kamiya et al., 1991; Burgess et al., 1991; Mastronarde et al., 1992; Muto et al., 1991; King et al., 1994; Piperno and Ramanis, 1991; LeDizet and Piperno, 1995). In contrast, the outer arm dyneins are homogeneous in composition and structural organization (Witman, 1992; Porter, 1996; Dutcher, 1995). The complexity of the inner row of dynein arms is illustrated by the numerous heavy chain subunits and associated proteins, each located in a distinct inner arm structure. Current models suggest that the inner arms are organized in precise groups that repeat in a 96-nm pattern, in exact register with the paired radial spokes and the drc structures (Witman, 1992; Dutcher, 1995; Porter, 1996). This organization was defined, in part, by *Chlamydomonas* mutants missing subsets of inner arm dynein components.

We took advantage of these dynein mutants, missing selected subsets of dynein components, to identify the critical inner arm dynein component, and predicted that double mutant axonemes missing both radial spokes and the regulatory phosphoprotein would no longer respond to PKI. Among the inner dynein arms is a structure referred to as inner arm I1 that is located in the proximal portion of each 96-nm repeat, composed of two heavy chains and three intermediate chain subunits with masses of 140, 138, and 97 kD, and can be isolated as a 21S particle or in the "f" fraction separated by Mono-Q chromatography (Goodenough et al., 1987; Kamiya et al., 1991; Smith and Sale, 1991; Porter et al., 1992; Kagami and Kamiya, 1992; Kato et al., 1993; Gardner et al., 1994). This inner arm dynein is defined by mutations in three loci referred to as *ida*1 (*pf9* or *pf30*), *ida*2, and *ida*3 (Brokaw and Kamiya, 1987; Piperno et al., 1990; Kamiya et al., 1991; Smith and Sale, 1991; Porter et al., 1992). We found that mutants missing both I1 and the radial spokes failed to respond to PKI. In contrast, mutants missing radial spokes and other dynein components responded to PKI in the same fashion as control axonemes missing only the radial spokes. We concluded inner arm I1 is required for PKI-induced increase in microtubule sliding and therefore predicted I1 contains a regulatory phosphoprotein. The 138-kD intermediate chain is the only phosphoprotein in I1. Coincident with increased dynein activity, phosphorylated 138-kD protein becomes selectively dephosphorylated upon rebinding to axonemes with wild-type radial spokes. We concluded that the radial spokes control I1's microtubule sliding activity by regulating the phosphorylation of the 138-kD intermediate chain. We predict regulation of I1's microtubule sliding is responsible for change in waveform. This prediction is supported by the studies of King and Dutcher (1997) that revealed that a new class of mutants, defective for phototaxis, has an altered pattern of phosphorylation in the 138-kD intermediate chain of I1.

Materials and Methods

Cell Strains, Growth Conditions, and Isolation of Double Mutants

Chlamydomonas reinhardtii strains studied include: 137c (wild type), *pf*17 (lacks radial spoke head, paralyzed), *pf*14 (lacks radial spoke, paralyzed), *pf*28 (lacks outer arm dynein, motile), double mutant *pf*28*pf*30 (lacking outer arm dynein and I1 inner arm dynein, paralyzed), *pf*14*pf*28 (lack radial spokes and outer arm dynein, paralyzed), *pf*14*pf*30 (*pf*14*ida*1, lack radial spokes and I1 inner arm dynein, paralyzed), *pf*17*ida*2 (lack radial spoke head and I1 inner arm dynein, paralyzed), *pf*17*ida*3 (lack radial spoke head and I1 inner arm dynein, paralyzed), and *pf*17*ida*4 (lack radial spoke head and subset of inner arm dynein components, paralyzed). Double mutant cells were either isolated from nonparental ditypes (*pf*17*ida*1, *pf*17*ida*2, *pf*17*ida*3, *pf*17*ida*4) or were generously provided by G. Piperno (Mount Sinai School of Medicine, New York) (*pf*14*pf*30). The phenotype of each cell type was verified by light and electron microscopy. With the exception of *pf*14*pf*28 cells, all strains were grown in liquid modified Medium I of Sager and Granick (1953), with aeration and a 14-h/10-h light/dark cycle (Witman, 1986). Due to an inability of the *pf*14*pf*28 to grow flagella of sufficient length in liquid culture, these cells were grown on agar plates (made in modified Medium I with Bacto-Agar; Difco Laboratories, Detroit, MI), at 22°C and over a 14-h/10-h light/dark cycle for 5–7 d. On the morning of an experiment, *pf*14*pf*28 cells were gently scraped and resuspended into 10 mM Hepes, pH 7.4 (10 ml per plate), and the cell suspension was maintained in light for 1 h. This procedure induced *pf*14*pf*28 cells to grow half-length flagella (Kurimoto and Kamiya, 1991; Habermacher and Sale, 1996).

Reagents, Phosphatase Inhibitors, and PKI[6-22] Amide

Radioactive labeling of isolated axonemes was performed using either [γ-^{32}P]ATP (Amersham Corp., Arlington Heights, IL) or [^{35}S]ATPγS (DuPont-New England Nuclear, Boston, MA). Microcystin-LR (Calbiochem-Novabiochem Corp., La Jolla, CA) was stored as a 500 μM stock in 10% MeOH at −20°C. PKI(6-22) amide (referred to here as PKI) is a peptide with the sequence Thr-Tyr-Ala-Asp-Phe-Ile-Ala-Ser-Gly-Arg-Thr-Gly-Arg-Arg-Asn-Ala-Ile-NH_2 that corresponds to residues 6–22 of the α isoform of the heat-stable inhibitor protein of the cAMP-dependent kinase, and it was synthesized and purified as described before (Howard et al., 1994). PKI was stored as a 500 mM stock in water at −70°C. A 100 mM stock solution of ATPγS (adenosine-5′-O-[3-thiotriphosphate], tetralithium salt; Calbiochem-Novabiochem Corp.) was made in water, and aliquots were stored at −20°C. A 100 mM stock of ATP (Boehringer Mannheim Biochemicals, Indianapolis, IN) was made in Tris buffer, and aliquots were stored at −20°C. Except as noted, all other chemicals were from Sigma Chemical Co. (St. Louis, MO), and deionized water was used throughout.

Isolation of Axonemes and the Microtubule Sliding Assay

Flagella were isolated as described previously (Witman, 1986; Smith and Sale, 1992*b*) and resuspended in buffer A (10 mM Hepes, 5 mM $MgSO_4$, 1 mM DTT, 0.5 mM EDTA, 30 mM NaCl, 0.1 mM PMSF, and 0.6 TIU Aprotinin, pH 7.4). Protein concentration was measured with the protein reagent (Bio Rad Laboratories, Richmond, CA). For demembranation and axoneme isolation, flagella were adjusted to 0.85 mg/ml, with a final

detergent concentration of 0.5% NP-40 (Calbiochem-Novabiochem Corp.). Axonemes were then pelleted at 37,000 *g* (18,000 rpm; SS-34 rotor [Sorvall Instruments Division, DuPont Co., Newton, CT]) for 20 min. The pelleted axonemes were resuspended to their previous volume in buffer B (10 mM Hepes, 5 mM $MgSO_4$, 1 mM DTT, 1 mM EGTA, 50 mM potassium acetate, 0.1 mM PMSF, 0.6 TIU Aprotinin, and 0.5% polyethylene glycol). Axonemes (~0.7 mg/ml) were then divided equally into the desired number of 1.5-ml Eppendorf tubes. As appropriate, PKI (100 nM) or buffer solvent was then added to the axonemes and incubated for 15 min on ice. The sample was supplemented with 1 mM ATP, or in some cases ATPγS (see below), followed by a 10-min incubation at room temperature. Microtubule sliding was then measured in 1 mM ATP as described before (Habermacher and Sale, 1996).

Extraction, Reconstitution, and Purification of Inner Dynein Arms

Inner arm dynein was extracted and reconstituted in vitro as described (Smith and Sale, 1992*a*,*b*; Habermacher and Sale, 1996). Dynein was isolated from either *pf*28 or *pf*14*pf*28 axonemes using one of two methods: axonemes were suspended in buffer A (~5 mg/ml) with either 1 mM ATP or 1 mM ATPγS before extraction of dynein. In some cases described below, radiolabeled ATP or ATPγS were used. Axonemes were then pelleted (18,000 rpm, 20 min, Sorvall SS-34 rotor), supernatants were removed, and axonemes were extracted in high salt buffer (0.6 M NaCl, 10 mM Hepes, 5 mM $MgSO_4$, 1 mM DTT, 0.5 mM EDTA, 0.1 mM PMSF, and 0.6 TIU Aprotinin) at a protein concentration of 8 mg/ml, for 20 min on ice. Dynein-containing supernatants were collected and dialyzed (molecular weight cutoff 12,000–14,000) twice in 500 ml of buffer A for 30 min at 4°C. I1 inner arm dynein was purified by sucrose density gradient sedimentation, and S-values were calculated as described previously (Piperno et al., 1990).

For reconstitution experiments, *pf*28*pf*30 axonemes were isolated and resuspended to 2 mg/ml in buffer A. As appropriate, microcystin-LR (2 μM) was added to *pf*28*pf*30 axonemes 15 min before reconstitution with extracts or purified I1 (Habermacher and Sale, 1996). Extracts of inner arm dynein or purified I1 fractions were mixed with an equal volume of isolated *pf*28*pf*30 axonemes: this ratio resulted in a four- to fivefold excess of dynein (Smith and Sale, 1992*b*). After incubating for 25 min on ice, the velocity of microtubule sliding was measured for controls and reconstituted axonemes.

In Vitro Radioactive Labeling of Radial Spoke–defective Axonemes

*pf*14*pf*28 axonemes were suspended in buffer A at a protein concentration of 5 mg/ml. In ^{32}P-labeling experiments, a mixture of [γ-^{32}P]ATP and unlabeled ATP was added to the *pf*14*pf*28 axonemes, resulting in a final ATP concentration of 100 μM with a sp act of 100 μCi/ml. In ^{35}S-labeling experiments, a 12.5 mM stock of [^{35}S]ATPγS was diluted 100-fold into *pf*14*pf*28 axoneme samples, to a final [^{35}S]ATPγS concentration of 125 μM with a sp act of 125 μCi/ml. Axonemes were incubated on ice for 15 min, followed by a 5-min incubation at room temperature. Axonemes were pelleted (15,000 rpm, 20 min, sorvall SS-34 rotor) through a sucrose pad (buffer A with 25% sucrose [wt/vol] and resuspended in high salt buffer (0.6 M NaCl, 10 mM Hepes, 5 mM $MgSO_4$, 1 mM DTT, 0.5 mM EDTA, 0.1 mM PMSF, and 0.6 TIU Aprotinin) at a protein concentration of 8–10 mg/ml. Labeled axonemes were extracted in high salt for 20 min, and subsequent fractionation steps were identical to those described above for unlabeled extract.

Gel Electrophoresis, Autoradiography, and Phosphorimage Analysis

For gel electrophoresis, samples were separated in 2–5% acrylamide and 0–8 M urea as described earlier (Smith and Sale, 1991). Gels were stained with Coomassie brilliant blue or in some cases were silver stained (Blum et al., 1987). For radioactive samples, dried gels were either exposed on a phosphorimager screen, x-ray film, or both. Quantitation of phosphorimager data was performed using the PhosphorImager SI (Molecular Dynamics, Sunnyvale, CA) and ImageQuaNT software (Molecular Dynamics). To ensure objective comparison of the radioactivity present in control and microcystin-LR–treated lanes, radioactive counts were measured through the full width of the lane, and as a function of position along the length of the lane. Total counts were plotted as a function of position.

Protein Quantitation by Densitometry

Sucrose gradient samples of I1 fractions were separated in 2–5% acrylamide and 0–8 M urea (Smith and Sale, 1991). Incrementally increasing amounts of purified phosphorylase B (100 ng increments, 100 ng to 1.2 μg) were separated in the 10 lanes adjacent to the I1 samples. Gels were stained with Coomassie brilliant blue, and densitometry was performed using Image 1 software (Universal Imaging Corp., West Chester, PA). A standard curve was plotted with known amounts of phosphorylase B, and this was used to estimate the amount of protein contained in the 138- and 140-kD intermediate chain bands.

Results

Inner Arm Dynein I1 is Required for PKI-induced Increase in Dynein Activity

To identify the dynein subunit required for regulation of microtubule sliding, we analyzed *Chlamydomonas* mutants lacking both the radial spokes as well as selected subsets of dynein components. As described above, this strategy has already revealed that the regulatory subunit is not found solely in the outer row of dynein arms, and therefore we focused our study on the inner row of dynein arms. Double mutants lacking both the radial spokes and selected subsets of inner arm dynein components were isolated from tetrads. Axonemes were isolated, and microtubule sliding velocities were measured in the presence and absence of the kinase inhibitor PKI. We predicted that a mutant axoneme missing the critical dynein component would no longer respond to addition of the kinase inhibitor PKI. The assumption was that the unknown regulatory phosphoprotein must be present, but present in a dephosphorylated form, for wild-type microtubule sliding (see Introduction and Fig. 1).

PKI treatment resulted in the expected increase in microtubule sliding in control axonemes missing the radial spokes (*pf*17 or *pf*14), central pair apparatus (*pf*18), or the double mutant lacking radial spokes as well as the outer row of dynein arms (*pf*14*pf*28) (Table I). Similarly, PKI treatment induced wild-type microtubule sliding in the double mutant (*pf*17*ida*4) lacking the radial spokes and the subset of inner arm dynein components missing in *ida*4 (Table I; Kamiya et al., 1991). In contrast, double mutants missing radial spokes and inner arm dynein I1 (*pf*14*pf*30, *pf*17*ida*1, 2, or 3) always failed to respond to PKI (Table I). We concluded I1 is required for PKI-induced increase in microtubule sliding velocity in spoke-defective axonemes. Therefore, we predicted that I1 contains a phosphoprotein subunit that regulates dynein's microtubule sliding activity.

138-kD Intermediate Chain Is Phosphorylated by an Axonemal Kinase

To determine if I1 contains candidate phosphoprotein subunits, axonemes missing the radial spokes were incubated with either [^{32}P]ATP or ATPγ^{35}S in the buffer used for motility. This approach was based on our previous results indicating that isolated axonemes, lacking radial spokes, retain the kinase activity that inhibits dynein (Howard et al., 1994). Therefore, axonemes from *pf*14*pf*28 were incubated with labeled ATP, the inner arm dyneins were extracted and fractionated, and the fractions were analyzed by SDS-PAGE, autoradiography, and phosphor-

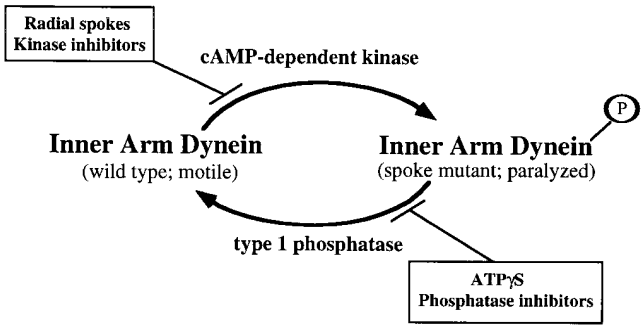

Figure 1. Model for regulation of *Chlamydomonas* flagellar dynein. Diverse physiological measurements indicate inner arm dynein's microtubule sliding activity is regulated by phosphorylation involving both an axonemal cAMP-dependent kinase and type-1 phosphatase (Habermacher and Sale, 1996). The data predicts an inner arm dynein component is phosphorylated in paralyzed axonemes lacking functional radial spokes, and that phosphorylation inhibits dynein's microtubule sliding activity. The model also predicts that the kinase inhibitor PKI can be used to block phosphorylation. Thus, to identify the component, PKI-induced change in microtubule sliding was measured in double mutants lacking both radial spokes and subsets of inner dynein arms. Based on this model, we predicted that microtubule sliding of axonemes missing the regulatory inner arm component would be unaffected by PKI.

imaging. Inner arm I1 sediments as a 21S particle composed of two heavy chains and three intermediate chains with nominal masses of 140, 138, and 97 kD (Fig. 2; Piperno et al., 1990; Kamiya et al., 1991; Smith and Sale, 1991; Porter et al., 1992). The corresponding phosphorimage revealed that, of the I1 subunits, only the 138-kD protein band and an associated, slower migrating protein smear (located between the 138- and 140-kD protein bands) incorporate phosphate. This is better viewed at higher magnification, comparing the pattern of Coomassie-stained protein with the phosphorimage of the same gel (Fig. 3). The 138-kD band forms a discrete band and contains the majority of the protein. Based on other evidence presented below, and data presented by King and Dutcher (1997), the highly phosphorylated protein smear appears to be a subfraction of the 138-kD protein that migrates more slowly because of phosphorylation at sites other than the phosphorylated residues in the discretely migrating 138-kD band. The same results were obtained when ATPγ^{35}S was used for labeling in place of [^{32}P]ATP. All I1 proteins and the radioactivity associated with them are completely absent in axonemes from mutant cells missing I1 (*pf*30 or *ida*1).

Using ^{32}P-labeled *pf*14*pf*28-21S fractions, as shown in Fig. 3 (fraction *18*), Coomassie blue staining, and a standard curve of protein generated with known amounts of phosphorylase B, the amount of protein in both the 140- and 138-kD band (*discrete lower band*) was calculated. Based on the calculated molar amounts of the two intermediate chains, the 138-kD band contains 7.4–25.6% fewer mol of protein than the 140-kD band (data not shown). Based on the assumption that the 140- and 138-kD intermediate chains are present at an equal stoichiometry (Pfister and Witman, 1984; King et al., 1996), these data suggest that 7.4–25.6% of the 138-kD intermediate chain is altered in its electrophoretic mobility, possibly as a result of hyperphosphorylation.

Wild-type Microtubule Sliding Requires Selective Dephosphorylation of Inner Arm I1

Change in phosphorylation of the 138-kD intermediate chain subunit is the simplest explanation for regulation of dynein's microtubule sliding activity. To test this theory, we predicted that reconstitution of phosphorylated I1 with axonemes bearing wild-type spokes would result in both selective dephosphorylation of the 138-kD intermediate chain and coincident increase in microtubule sliding velocity. The strategy is illustrated in Fig. 4, adapted from Smith and Sale (1992*b*), and involves mixing extracted inner arm dynein, or purified I1, with isolated axonemes specifically missing inner arm I1, as well as the outer arm dynein, but retaining wild-type radial spokes (*pf*28*pf*30). As described previously, in vitro reconstitution with these axonemes resulted in selective structural and functional restoration of I1 (Smith and Sale, 1992*b*). Therefore, after reconstitution

Table I. Dynein-driven Microtubule Sliding in Presence and Absence of PKI

Cell type	Missing structure	Control	+PKI	Percentage of change
				%
Wild-type	None	22.0 ± 1.5	21.8 ± 1.3	0.9
Single Mutants				
*pf*28	Outer dynein arm	7.5 ± 1.0	7.3 ± 0.9	2.6
*pf*14	Radial spoke	11.7 ± 0.9	17.2 ± 1.7	47.0*
*pf*17	Radial spokehead	13.7 ± 1.0	21.5 ± 1.5	57.5*
*pf*18	Central pair	12.0 ± 1.2	21.5 ± 1.4	79.2*
*ida*1	I1	21.4 ± 1.6	22.2 ± 1.6	4.0
*ida*4	I2 (subset of inner arms)	17.5 ± 0.8	18.1 ± 1.3	3.4
Double Mutants				
*pf*14*pf*28	Radial spoke and outer arm	3.5 ± 0.5	5.4 ± 0.8	54.3*
*pf*14*pf*30	Radial spoke and I1 arm	11.0 ± 0.8	10.7 ± 0.9	2.7
*pf*17*ida*2	Radial spoke and I1 arm	10.4 ± 1.6	10.2 ± 1.5	2.1
*pf*17*ida*3	Radial spoke and I1 arm	10.1 ± 0.8	10.1 ± 1.1	0.0
*pf*17*ida*4	Radial spoke and I2 arm	10.2 ± 1.3	17.0 ± 1.5	67.3*

*Denotes significant change between control and PKI-treated samples (*t* test, $P < 0.01$).

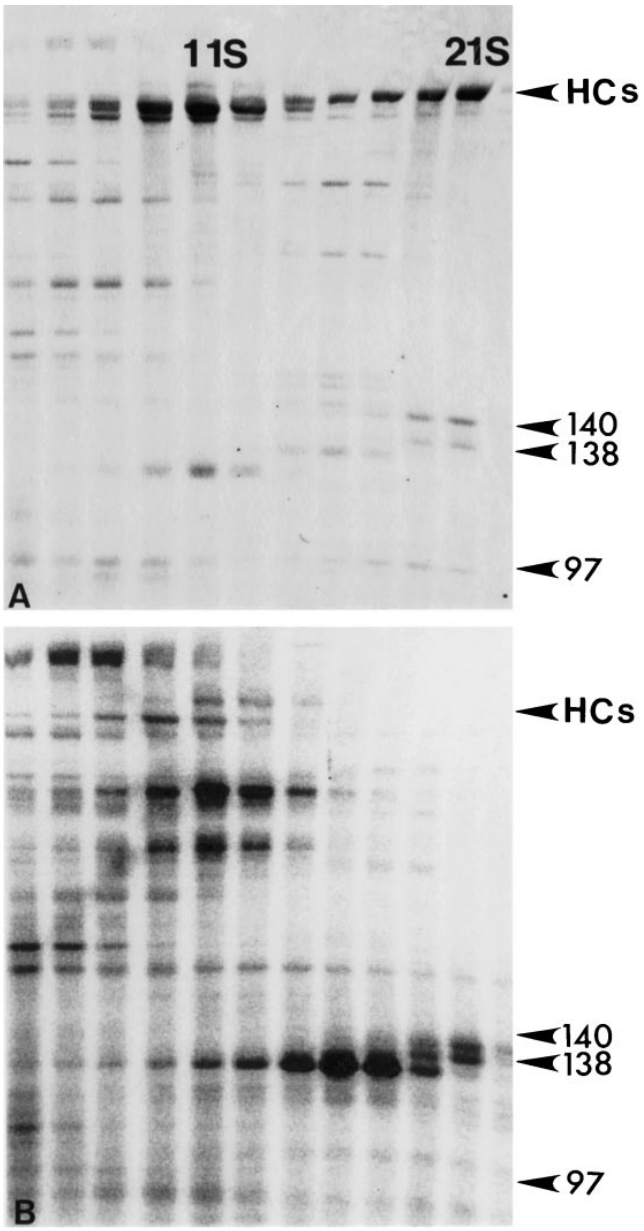

Figure 2. Electrophoretic separation of fractions from a portion of a sucrose gradient used to purify I1. The fractions were arranged with the direction of sedimentation from left to right. (*A*) Coomassie-stained SDS-PAGE electrophoretogram of *pf*14*pf*28 high salt extract. Inner arm I1 sediments as a 21S particle and is composed of two heavy chains (not resolved in this gel) and three intermediate chains with masses of 140, 138, and 97 kD. (*B*) The corresponding phosphorimage demonstrates that the 138-kD intermediate chain (and associated protein smear) is the only I1 component labeled. The same conclusions were drawn in parallel experiments using [^{35}S]ATPγS.

with axonemes bearing wild-type radial spokes, we tested whether the 138-kD intermediate chain specifically becomes dephosphorylated. In control experiments, we tested whether ATPγS treatment of I1 or addition of phosphatase inhibitors selectively block dephosphorylation and block induction of increased microtubule sliding velocity.

The velocity of dynein-driven microtubule sliding is

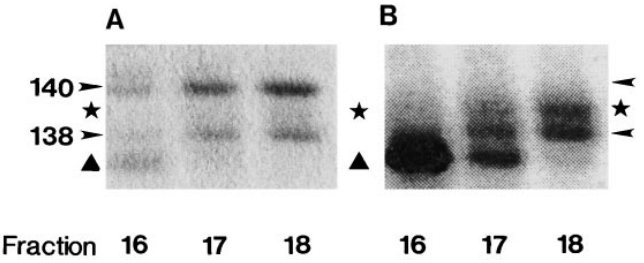

Figure 3. Higher magnification comparison of the (*A*) Coomassie staining and (*B*) ^{32}P-incorporation in the 138/140-kD molecular mass region of the I1 inner dynein arm reveals that the 138-kD intermediate chain and a minor smear of protein, migrating between the 140-kD intermediate chain and the 138-kD band (★), is phosphorylated. The 140-kD intermediate chain is not phosphorylated. A phosphorylated protein of 133 kD (▲) also sediments in the 21S region of the sucrose gradient, but is not a component of the I1 inner arm.

greatly reduced in axonemes missing inner arm I1: microtubules from control axonemes, lacking outer arms (*pf*28) slid at ~7.5 μm/s, whereas microtubules from *pf*28*pf*30 slid at ~4 μm/s (Fig. 5). Reconstitution of unfractionated inner arm dynein extracts, derived from either *pf*28 or *pf*14*pf*28, restored microtubule sliding to control velocity (Fig. 5, compare bars *4* and *5* with bar *1*; Smith and Sale, 1992*a*). In contrast, thiophosphorylation of the inner arm extract, before extraction or reconstitution, blocked increased microtubule sliding (Fig. 5, bar *6*). Addition of the phosphatase inhibitor microcystin-LR to the axonemes also prevented increased microtubule sliding (Fig. 5, bar *7*). The same results were obtained using purified inner arm I1 for reconstitution: the 21S fraction restored control microtubule sliding, and the phosphatase inhibitor microcystin-LR blocked restoration of control microtubule sliding (Fig. 6). Based on analysis by gel electrophoresis, neither thiophosphorylation nor phosphatase inhibitors altered the precision or specificity of structural rebinding of I1 to isolated axonemes (data not shown). Therefore, the lack of restored microtubule sliding activity, after these treatments, was specifically due to phosphorylation of I1.

Wild-type Microtubule Sliding Requires Dephosphorylation of the 138-kD Intermediate Chain

These results are consistent with a model in which dephosphorylation of a component of I1, probably the 138-kD intermediate chain, is required for wild-type dynein-driven motility. To test whether wild-type motility requires dephosphorylation of the 138-kD protein, isolated axonemes from *pf*14*pf*28 were incubated with [^{32}P]ATP to phosphorylate the inner arm dynein fraction before salt extraction. The labeled inner arm dynein fraction was then solubilized and either used directly for reconstitution or fractionated on sucrose gradients for purification of I1 before reconstitution. Reconstitution was performed as described above, either in the absence or presence of the phosphatase inhibitor microcystin-LR, using axonemes missing the outer dynein arms and inner arm I1 (*pf*28*pf*30). After reconstitution, axonemes were sedimented through a sucrose cushion and prepared for gel electrophoresis and phosphorimager analy-

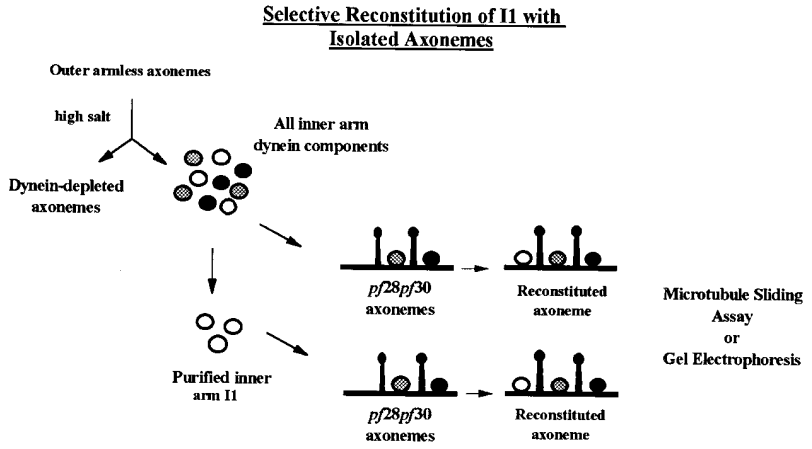

Figure 4. Strategy for selective reconstitution of inner arm I1 with axonemes from *pf*28*pf*30 that lack outer dynein arms and inner arm I1. Inner arm dyneins are solubilized from axonemes missing outer arms (*pf*28 or *pf*14*pf*28) and extracts used either directly for reconstitution or first used to purify I1 by sucrose gradient sedimentation. After reconstitution with *pf*28*pf*30 axonemes, axonemes were analyzed using the sliding disintegration assay or prepared for gel electrophoresis.

sis. The advantage of the first experiment, using the unfractionated extract, is that all radioactive proteins that rebind to the axoneme can be compared. We predicted that among the phosphoproteins that rebind to the isolated axonemes, only the critical component, presumably the 138-kD protein, would become dephosphorylated. Furthermore, we predicted the phosphatase inhibitor microcystin-LR would block dephosphorylation.

The results of this experiment are illustrated in Fig. 7, and, as predicted, recombination of the I1-containing extract with axonemes bearing radial spokes resulted in selective loss of radioactivity in the 138-kD intermediate

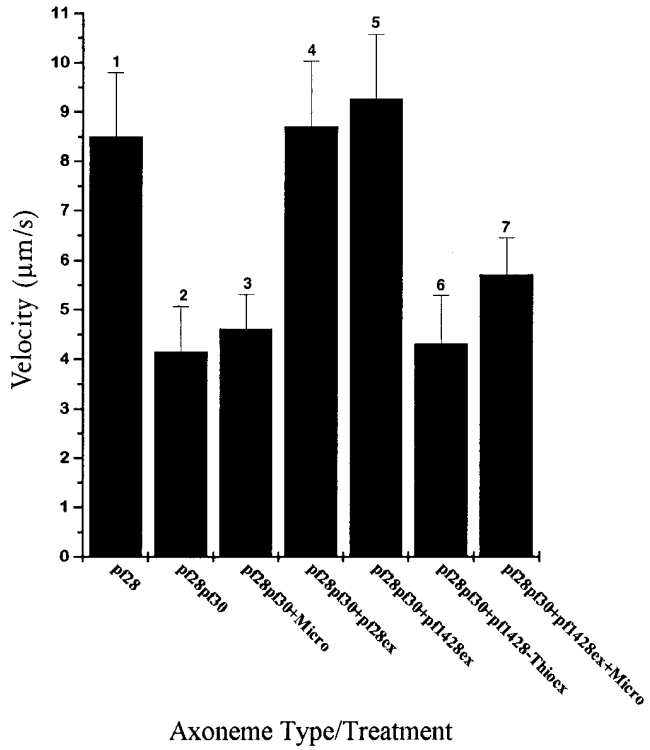

Figure 5. Restoration of wild-type inner arm microtubule sliding requires dephosphorylation of an I1 inner arm component. Sliding disintegration assay was performed on: (*1*) unextracted *pf*28 axonemes (*pf28*), (*2*) unextracted *pf*28*pf*30 axonemes (*pf28pf30*), (*3*) microcystin-LR–treated *pf*28*pf*30 axonemes (*pf28pf30+Micro*), (*4*) *pf*28 inner arm extract reconstituted onto *pf*28*pf*30 axonemes (*pf28pf30+pf28ex*), (*5*) pf14*pf*28 inner arm extract reconstituted onto *pf*28*pf*30 axonemes (*pf28pf30+pf1428ex*), (*6*) thiophosphorylated *pf*14*pf*28 inner arm extract reconstituted onto *pf*28*pf*30 axonemes (*pf28pf30+pf1428-Thioex*), and (*7*) pf14*pf*28 inner arm extract reconstituted onto microcystin-LR–treated *pf*28*pf*30 axonemes (*pf28pf30+pf1428ex+Micro*).

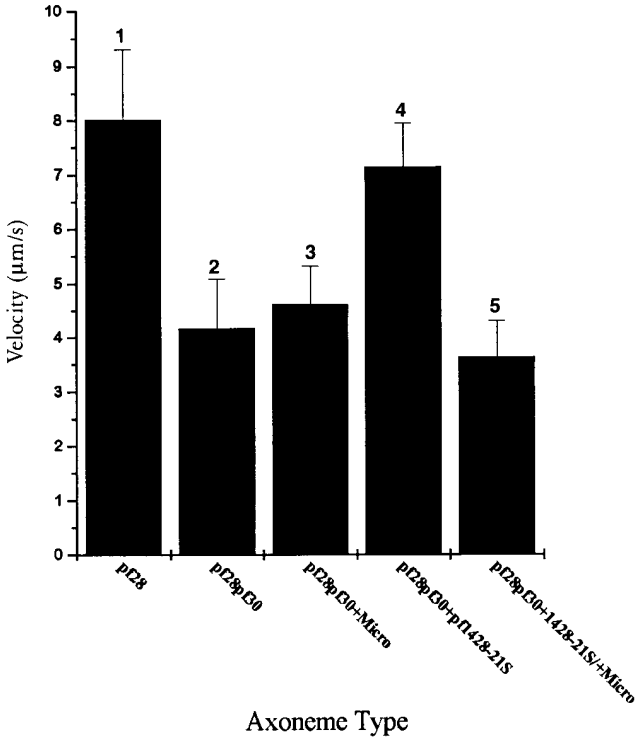

Figure 6. Dephosphorylation of isolated inner arm I1 is required for restoration of wild-type inner arm microtubule sliding. The sliding disintegration assay was performed on: (*1*) unextracted *pf*28 axonemes (*pf28*), (*2*) unextracted *pf*28*pf*30 axonemes (*pf28pf30*), (*3*) microcystin-LR–treated *pf*28*pf*30 axonemes (*pf28pf30+Micro*), (*4*) purified *pf*14*pf*28 inner arm I1 from a sucrose gradient reconstituted onto *pf*28*pf*30 axonemes (*pf28pf30+1428-21S*), and (*5*) purified *pf*14*pf*28 inner arm I1 from a sucrose gradient reconstituted onto microcystin-LR–treated *pf*28*pf*30 axonemes (*pf28pf30+1428-21S/+Micro*).

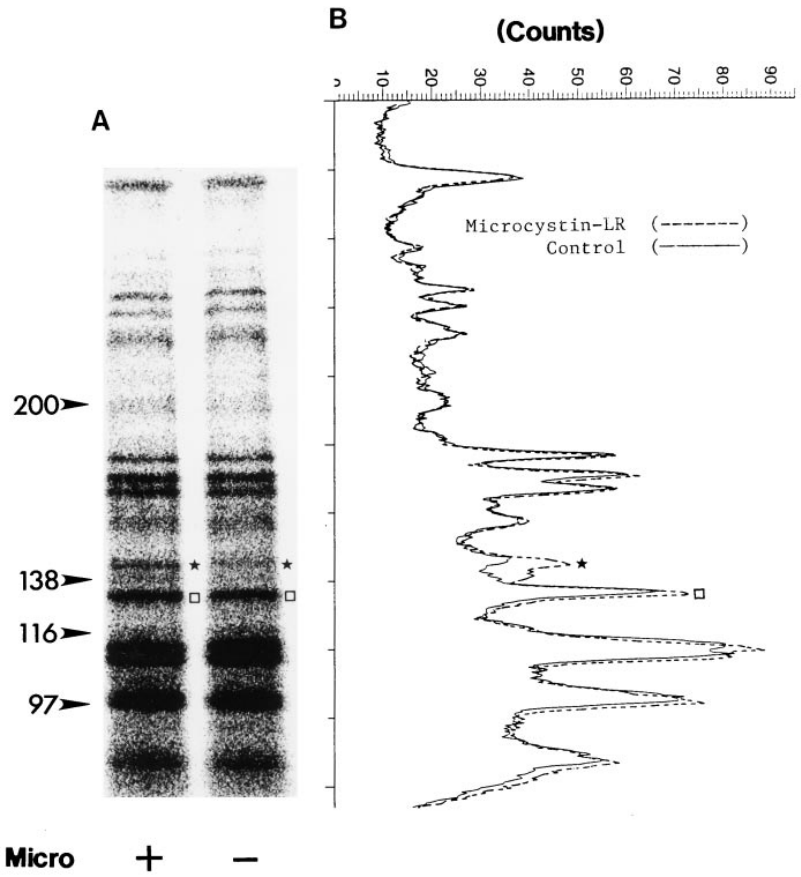

Figure 7. The 138-kD intermediate chain is selectively dephosphorylated after reconstitution of phosphorylated inner arm extracts with *pf*28*pf*30 axonemes. (*A*) Phosphorimage analysis of SDS-PAGE electrophoretogram of ^{32}P-labeled *pf*14*pf*28 high salt extract reconstituted with *pf*28*pf*30 axonemes in the presence (+) and absence (−) of microcystin-LR. (*B*) A comparison of the total counts in *A* as a function of protein position from top to bottom. The solid line (——) represents control labeling and the dashed line (-----) represents labeling in the presence of microcystin-LR. For comparison, a nondynein, ~130-kD phosphoprotein (□) is not affected by microcystin-LR after reconstitution. These data indicate that the region above the 138-kD intermediate chain (★), as well as the 138-kD intermediate chain itself, are selectively dephosphorylated after reconstitution with *pf*28*pf*30 axonemes.

chain proteins compared with the experimental fraction treated with microcystin-LR. In comparisons of phosphorimages of untreated and microcystin-LR-treated samples, the phosphate content in the 138-kD proteins is specifically affected (Fig. 7 *A*). However, as described below in more detail, the slower migrating fraction (★) of the 138-kD proteins appeared to lose a greater fraction of radioactivity compared with the fraction migrating with the 138-kD band. As illustrated in the accompanying graph (Fig. 7 *B*), phosphate content is not affected for any other protein and precisely the same phosphoproteins rebind to axonemes whether or not microcystin-LR was added. Analysis of Coomassie-stained gels indicated an equal amount of extracted proteins rebound to axonemes irrespective of addition of microcystin-LR (data not shown).

The same reconstitution experiment was repeated using purified I1. The results also revealed that, in the absence of microcystin-LR, reconstitution of I1 with radial spoke–bearing axonemes resulted in partial loss of radioactivity, predominantly from the upper, slower migrating fraction of the 138-kD proteins (Fig. 8). Again, analysis of Coomassie-stained gels indicated that the same amount of I1 proteins bound to the axoneme. The simplest interpretation of the data is that phosphorylation of inner arm I1 by an axonemal kinase results in selective phosphorylation of a fraction of the 138-kD intermediate chain and leads to a slower migration of the protein. Reconstitution of the I1 fraction with axonemes bearing radial spokes results in dephosphorylation of the 138-kD protein.

Discussion

Regulation of Flagellar Microtubule Sliding by Inner Arm Dynein I1 and Phosphorylation of the 138-kD Intermediate Chain

We previously demonstrated that flagellar dynein's microtubule sliding activity is regulated by the radial spokes and that the regulatory mechanism involves an axonemal cAMP-dependent kinase, type-I phosphatase, and an unknown inner arm dynein component (Habermacher and Sale, 1996; see Fig. 1). We now report that inner arm dynein subform I1 is a key element in regulation of flagellar microtubule sliding activity. I1 is required for PKI-induced increase in microtubule sliding velocity. For all mutant axonemes in which I1 was missing, microtubule sliding velocity did not change after addition of PKI (Table I). The simplest interpretation is that I1 is required for changes in microtubule sliding and that the crucial alteration to I1 involves change in phosphorylation of a regulatory subunit. This conclusion is supported, in part, by reconstitution experiments in which ATPγS pretreatment of inner arm dynein extracts, before the reconstitution with axonemes specifically lacking I1, blocks restoration of wild-type microtubule sliding. This inhibition of sliding occurs despite the presence of wild-type radial spokes, and suggests that dephosphorylation of I1 is required for restoration of wild-type microtubule sliding. Therefore, we focused exclusively on analysis of I1 and assessed the phosphorylation

of I1 proteins under conditions used for measurement of microtubule sliding.

Discovery that I1 is a key regulatory element for flagellar motility is consistent with the earlier observation that alterations in I1, or assembly of I1, can suppress paralysis in flagellar mutants with defective central pair apparatus (Porter et al., 1992). Furthermore, the magnitude of PKI-induced increase in the velocity of microtubule sliding, in axonemes containing outer arm dynein but missing the spokes, indicates outer arm dynein activity is also regulated by change in phosphorylation of an axonemal component. We do not know whether outer arm activity is independently regulated as demonstrated by others (Hamasaki et al., 1989, 1991; Barkalow et al., 1994; see also King and Witman, 1994; King and Patel-King, 1995). However, it is clear that PKI-induced effects on outer arm activity, in the absence of radial spokes, require the presence of inner arm dynein I1 (Table I). It is possible I1 alters outer arm dynein activity through mechanical interaction.

To determine physiologically significant sites of phosphorylation, axonemes lacking radial spokes were incubated in either [^{32}P]ATP or ATPγ^{35}S in motility buffer. Paralyzed, spoke-defective axonemes were used based upon the hypothesis that microtubule sliding is inhibited in these axonemes as a result of phosphorylation of the critical inner dynein arm component (Habermacher and Sale, 1995, 1996; Fig. 1). Therefore, we predicted paralyzed axonemes would contain the phosphorylated regulatory protein. The only I1 subunit to become phosphorylated, or thiophosphorylated, under these conditions was the 138-kD intermediate chain. The 138-kD subunit always copurified with other I1 subunits as a 21S sedimenting particle or in the "f" fraction separated by Mono-Q chromatography, and it was missing in isolated axonemes in *ida*1, *ida*2, and *ida*3 (compare with Goodenough et al., 1987; Kamiya et al., 1991; Smith and Sale, 1991; Porter et al., 1992; Gardner et al., 1994). Thus, the evidence is compelling that the 138-kD phosphoprotein is an intermediate chain of I1, as well as the only phosphoprotein subunit.

Phosphorylation of the 138-kD protein appears to be complex and results in change in migration of a subset of the protein when analyzed by SDS-PAGE. As illustrated in Fig. 2 and discussed in the studies by King and Dutcher (1997), most of the protein of 138 kD runs as a discrete band with a nominal mass of 138 kD. However, a smaller, minor fraction migrates more slowly as a smear of highly phosphorylated protein. As described in Results, and assuming equal stoichiometry of the intermediate chains, quantitative comparison of the molar fraction of the 140- and 138-kD intermediate chains by densitometry indicated that ~10% of the 138-kD protein from *pf*14*pf*28 axonemes may migrate with altered electrophoretic mobility. The simplest interpretation is that the electrophoretic migration of this subset of 138 kD is altered by phosphorylation. Consistent with this interpretation is the observation that in vitro treatment of the fraction with various phosphatases results in loss of the minor, slowly migrating component with a corresponding increase in the amount of protein in the 138-kD band (King and Dutcher, 1997). In preliminary studies, we also found that the amount of protein in the discretely migrating 138-kD band is increased upon treatment of the 21S fraction with a purified type-1 phosphatase. Furthermore, reconstitution experiments using ^{32}P-labeled 138 kD resulted in a greater loss in radioactivity in the slower migrating fraction compared with that of the 138-kD band (Fig. 8).

Together, these data indicate that the slowly migrating fraction of the 138 kD is a consequence of phosphorylation of additional specialized residues. The pattern of dephosphorylation induced by recombination with axonemes bearing radial spokes, and the corresponding changes in dynein activity, suggest that the highly phosphorylated minor fraction is responsible for inhibition of microtubule sliding. Based on the scheme proposed in Fig. 1, dephosphorylation of these residues must occur for wild-type microtubule sliding or induction of wild-type motility. Consistent with this model is the observation that wild-type axonemes do not display a prominent smear of protein above the 138-kD band (King and Dutcher, 1997). These results suggest that a relatively small amount of highly phosphorylated 138-kD protein, found in the smeared region above the 138-kD band, is sufficient to inhibit flagellar dynein activity throughout the axoneme. It is possible that small numbers of phosphorylated I1, distributed evenly among the doublet microtubules, are sufficient to alter the activity of the remaining flagellar dyneins: we have never observed graded microtubule sliding velocity (see Hamasaki et al., 1995). Alternatively, it is possible that a phosphorylated subset of I1 is asymmetrically distributed along or among the doublet microtubules or between the *cis* and *trans* flagella. Localization of the phosphorylated subset of I1 will distinguish these possibilities. The distinguishing feature of this subset of I1 may be the location of the kinase and phosphatase that regulate I1. For example, although I1 may be evenly distributed throughout the axoneme, these regulatory enzymes may be associated with only a select subset of I1 complexes (see Discussion below).

In vitro microtubule translocation assays using purified I1 may also help to distinguish models that show how phosphorylated I1 alters microtubule sliding. However, use of such assays with purified I1 has resulted in either failure of movement or translocation of microtubules at

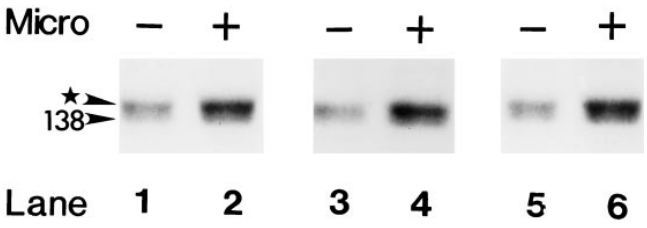

Figure 8. The 138-kD intermediate chain is dephosphorylated after reconstitution of labeled purified I1 with *pf*28*pf*30 axonemes. (Lanes *1–6*) Autoradiograph of three separate experiments in which ^{32}P-labeled 21S fraction from *pf*14*pf*28 was reconstituted onto *pf*28*pf*30 axonemes in the presence (lanes *2*, *4*, and *6*) and absence (lanes *1*, *3*, and *5*) of microcystin-LR. The shifted region above the 138-kD intermediate chain (★) and the 138-kD intermediate chain itself are the only phosphoproteins in the 21S fraction that bind to *pf*28*pf*30 axonemes. The shifted region above the 138-kD intermediate chain (★) is greatly dephosphorylated after reconstitution with *pf*28*pf*30 axonemes, and this dephosphorylation is blocked by microcystin-LR.

velocities significantly slower than all other isolated dyneins (Smith and Sale, 1991; Kagami and Kamiya, 1992). In vitro microtubule translocation assays may not be appropriate for the analysis of isolated I1. However, based on the results reported in this paper, it is also possible that I1 failed to induce microtubule translocation because of phosphorylation of the 138 kD.

Structural Association of the Axonemal Kinase and Phosphatase with Inner Arm I1

The in vitro measurement of dynein-driven microtubule sliding using isolated axonemes indicated the cAMP-dependent kinase and type-1 phosphatase are tightly associated with the axoneme (Howard et al., 1994; Habermacher and Sale, 1996). The basis for this conclusion includes physiological studies of isolated, washed axonemes in which all membrane and matrix components are removed before assay. Predictably, therefore, the regulatory subunit must be structurally associated with the catalytic domain of the kinase and phosphatase.

One hypothesis, based on structural and biochemical analysis of the 78-kD intermediate chain of the outer dynein arm (King and Witman, 1990; King et al., 1991), is that the 138-kD intermediate chain is located at the site at which I1 attaches to the doublet microtubule. This position is in close proximity to the base of the radial spokes and the drc (Piperno et al., 1992, 1994; Gardner et al., 1994). Therefore, predictably the kinase and/or the phosphatase are components of or closely associated with the spokes or the drc, exactly in position to affect changes in phosphorylation of the 138-kD intermediate chain. As described above, the kinase and phosphatase may be associated with only a subset of I1 complexes located in functionally significant positions along or among the flagellar microtubules. We are currently testing this hypothesis.

Physiological Role of I1 for Flagellar Motility

Although these data strongly indicate that flagellar dynein activity can be regulated by the radial spokes and through change in phosphorylation of the 138-kD intermediate chain, the relationship of changes in microtubule sliding to flagellar bending remains unclear. The microtubule sliding assay does not directly address the role of the radial spokes or I1 in flagellar motility. However, based on studies of others, we postulate that the radial spokes and inner dynein arms play a role in regulation of waveform (Brokaw and Kamiya, 1987; Brokaw, 1994). A variety of observations indicate a specialized role for I1 in the regulation of motility. First, in mutants lacking I1, waveform is modified compared with that of wild type (Brokaw and Kamiya, 1987). Second, in the absence of outer arms, microtubule sliding velocity is greatly reduced when I1 is missing (Kurimoto and Kamiya, 1991; Smith and Sale, 1992*b*). Third, microtubule translocation, induced in vitro with purified I1, is ineffective compared with dynein from other sources (Smith and Sale, 1991; Kagami and Kamiya, 1992). Fourth, mutations in I1 suppress paralysis of certain central pair mutants (Porter et al., 1992).

These data are consistent with a model in which changes in waveform are a consequence of modification of the pattern of microtubule sliding (Brokaw and Kamiya, 1987; Brokaw, 1994; Kamiya, 1995). Predictably, modulation of I1's microtubule sliding activity plays a central role. I1 activity also appears to be involved in a signal cascade that results in waveform changes during phototaxis. The basis for this conclusion includes results from King and Dutcher (1997) in the study of behavioral mutants that failed to properly undergo phototaxis. Using a sensitive fractionation procedure, King and Dutcher (1997) discovered in some of these mutants that the migration of the 138-kD intermediate chain is modified and that modification can be overcome by treatment of the fraction with phosphatases. The simplest model is that, in the sequence of events leading to modification of waveform, changes in phosphorylation of the 138-kD intermediate chain are a required step. Diverse and compelling evidence also indicates that flagellar waveform in *Chlamydomonas* is regulated by calcium (Bessen et al., 1980; Omoto and Brokaw, 1985). The mechanism for calcium-induced changes is not understood. However, based on data that I1 plays a role in regulation of waveform, it is possible that calcium affects the state of phosphorylation of the 138-kD intermediate chain. The mechanism could either involve direct effects of calcium on I1 or on the enzymes that modulate phosphorylation of the 138-kD subunit or a cascade involving other enzymes (Tash and Bracho, 1994; Walzak and Nelson, 1994; Chaudhry et al., 1995).

We gratefully acknowledge Dr. David Howard for the helpful discussion and experimental advice. We thank Drs. Elizabeth Smith, Lynne Quarmby, and Pinfen Yang for discussion of the manuscript, and Drs. Stephen J. King and Susan K. Dutcher for sharing their data.

The work reported here was supported by a grant from the National Institutes of Health (GM51173).

Received for publication 6 September 1996 and in revised form 29 October 1996.

References

Barkalow, K., T. Hamasaki, and P. Satir. 1994. Regulation of 22S dynein by a 29-kD light chain. *J. Cell Biol.* 126:727–735.

Bessen, M., R.B. Fay, and G.B. Witman. 1980. Calcium control of waveform on isolated flagellar axonemes of *Chlamydomonas. J. Cell Biol.* 86:446–455.

Blum, H., H. Beier, and B. Huang. 1987. Improved silver staining of plant proteins, RNA and DNA in polyacrylamide gels. *Electrophoresis.* 8:93–97.

Brokaw, C.J. 1994. Control of flagellar bending: a new agenda based on dynein diversity. *Cell Motil. Cytoskeleton.* 28:199–204.

Brokaw, C.J., and R. Kamiya. 1987. Bending patterns on *Chlamydomonas* flagella. IV. Mutants with defects in inner and outer arms indicate differences in dynein arm function. *Cell Motil. Cytoskeleton.* 8:68–75.

Brokaw, C.J., D.J.L. Luck, and B. Huang. 1982. Analysis of the movement of *Chlamydomonas* flagella: the function of the radial spoke system is revealed by comparison of wild-type and mutant flagella. *J. Cell Biol.* 92:722–732.

Burgess, S.A., D.A. Carter, S.D. Dover, and D.M. Woolley. 1991. The inner dynein arm complex: compatible images from freeze-etch and thin section methods of microscopy. *J. Cell Sci.* 100:319–328.

Chaudhry, P.S., S. Creagh, N. Yu, and C.J. Brokaw. 1995. Multiple protein kinase activities required for activation of sperm flagellar motility. *Cell Motil. Cytoskeleton.* 32:65–79.

Curry, A.M., and J.L. Rosenbaum. 1993. Flagellar radial spoke: a model molecular genetic system for studying organelle assembly. *Cell Motil. Cytoskeleton.* 24:224–232.

Dutcher, S.K. 1995. Flagellar assembly in two hundred and fifty easy-to-follow steps. *Trends Genet.* 11:398–404.

Gardner, L.C., E. O'Toole, C.A. Perrone, T. Giddings, and M.E. Porter. 1994. Components of a "Dynein Regulatory Complex" are located at the junction between the radial spokes and the dynein arms in *Chlamydomonas* flagella. *J. Cell Biol.* 127:1311–1325.

Goodenough, U.W., and J.E. Heuser. 1984. Structural comparison of purified proteins with *in situ* dynein arms. *J. Mol. Biol.* 180:1083–1118.

Goodenough, U.W., B. Gebhart, V. Memall, D.R. Mitchell, and J.E. Heuser. 1987. HPLC fractionation of *Chlamydomonas* dynein extracts and characterization of inner arm dynein subunits. *J. Mol. Biol.* 194:481–494.

Habermacher, G., and W.S. Sale. 1995. Regulation of dynein-driven microtubule sliding by an axonemal kinase and phosphatase in *Chlamydomonas* flagella. *Cell Motil. Cytoskeleton.* 32:106–109.

Habermacher, G., and W.S. Sale. 1996. Regulation of flagellar dynein by an axonemal type 1 phosphatase in *Chlamydomonas*. *J. Cell Sci.* 109:1899–1907.

Hamasaki, T., T.J. Murtaugh, B.H. Satir, and P. Satir. 1989. *In vitro* phosphorylation of *Paramecium* axonemes and permeabilized cells. *Cell Motil. Cytoskeleton.* 12:1–11.

Hamasaki, T., K. Barkalow, J. Richmond, and P. Satir. 1991. cAMP-stimulated phosphorylation of an axonemal polypeptide that copurifies with the 22S dynein arm regulates microtubule translocation velocity and swimming speed in *Paramecium*. *Proc. Natl. Acad. Sci. USA*. 88:7918–7922.

Hamasaki, T., M.E.J. Holwill, K. Barkalow, and P. Satir. 1995. Mechanochemical aspects of axonemal dynein activity studied by *in vitro* microtubule translocation. *Biophys. J.* 69:2569–2579.

Hasegawa, E., H. Hayashi, S. Asakura, and R. Kamiya. 1987. Stimulation of *in vitro* motility of *Chlamydomonas* axonemes by inhibition of cAMP-dependent phosphorylation. *Cell Motil. Cytoskeleton.* 8:302–311.

Howard, D., G. Habermacher, D.B. Glass, E.F. Smith, and W.S. Sale. 1994. Regulation of *Chlamydomonas* flagellar dynein by an axonemal protein kinase. *J. Cell Biol.* 127:1683–1692.

Huang, B. 1986. *Chlamydomonas reinhardtii*: a model system for the genetic analysis of flagellar structure and motility. *Int. Rev. Cytol.* 99:181–215.

Huang, B., Z. Ramanis, and D.J.L. Luck. 1982. Suppressor mutations in *Chlamydomonas* reveal a regulatory mechanism for flagellar function. *Cell.* 28:115–124.

Kagami, O., and R. Kamiya. 1992. Translocation and rotation of microtubules caused by multiple species of *Chlamydomonas* inner arm dynein. *J. Cell Sci.* 103:653–664.

Kamiya, R. 1995. Exploring the function of inner and outer dynein arms with *Chlamydomonas* mutants. *Cell Motil. Cytoskeleton.* 32:98–102.

Kamiya, R., E. Kurimoto, and E. Muto. 1991. Two types of *Chlamydomonas* flagellar mutants missing different components of inner arm dynein. *J. Cell Biol.* 112:441–447.

Kato, T., O. Kagami, T. Yagi, and R. Kamiya. 1993. Isolation of two species of *Chlamydomonas reinhardtii* flagellar mutants, *ida*5 and *ida*6, that lack a newly identified heavy chain of inner dynein arm. *Cell Struct. Funct.* 18:371–377.

King, S.J., and S.K. Dutcher. 1997. Phosphoregulation of an inner dynein arm complex in *Chlamydomonas reinhardtii* is altered in phototactic mutant strains. *J. Cell Biol.* 136:177–191.

King, S.J., W. Inwood, E. O'Toole, J. Power, and S.K. Dutcher. 1994. The *bop2-1* mutation reveals radial asymmetry in the inner dynein arm region of *Chlamydomonas reinhardtii*. *J. Cell Biol.* 126:1255–1266.

King, S.M., and R.S. Patel-King. 1995. Identification of a Ca^{2+}-binding light chain within *Chlamydomonas* outer arm dynein. *J. Cell Sci.* 108:3757–3764.

King, S.M., and G.B. Witman. 1990. Localization of an intermediate chain of outer arm dynein by immunoelectron microscopy. *J. Biol. Chem.* 265:19807–19811.

King, S.M., and G.B. Witman. 1994. Multiple sites of phosphorylation within the α-heavy chain of *Chlamydomonas* outer arm dynein. *J. Biol. Chem.* 269: 5452–5457.

King, S.M., C.G. Wilkerson, and G.B. Witman. 1991. The M_r 78,000 intermediate chain of *Chlamydomonas* outer arm dynein interacts with α-tubulin *in situ*. *J. Biol. Chem.* 266:8401–8407.

King, S.M., E. Barbarese, J.F. Dillman III, R.S. Patel-King, J.H. Carson, and K.K. Pfister. 1996. Brain cytoplasmic and flagellar outer arm dyneins share a highly conserved M_r 8,000 light chain. *J. Biol. Chem.* 271:19358–19366.

Kurimoto, E., and R. Kamiya. 1991. Microtubule sliding in flagellar axonemes of *Chlamydomonas* mutants missing inner or outer arm dynein: velocity measurements on new types of mutants by an improved method. *Cell Motil. Cytoskeleton.* 19:275–281.

LeDizet, M., and G. Piperno. 1995. The light chain p28 associates with a subset of inner dynein arm heavy chains in *Chlamydomonas* axonemes. *Mol. Biol. Cell.* 6:697–711.

Mastronarde, D., E. O'Toole, K. McDonald. J.R. McIntosh, and M. Porter. 1992. Arrangement on inner dynein arms in wild-type and mutant flagella of *Chlamydomonas*. *J. Cell Biol.* 118:1145–1162.

Muto, E., R. Kamiya, and S. Tsukita, 1991. Double rowed organization of inner dynein arms in *Chlamydomonas* flagella revealed by tilt series thin section electron microscopy. *J. Cell Sci.* 99:57–66.

Omoto, C.K., and C.J. Brokaw. 1985. Bending patterns of *Chlamydomonas* flagella. II. Calcium effects on reactivated *Chlamydomonas* flagella. *Cell Motil. Cytoskeleton.* 5:53–60.

Pfister, K.K., and G.B. Witman. 1984. Subfractionation of *Chlamydomonas* 18S dynein into two unique subunits containing ATPase activity. *J. Biol. Chem.* 259:12072–12080.

Piperno, G. 1995. Regulation of dynein activity within *Chlamydomonas* flagella. *Cell Motil. Cytoskeleton.* 32:103–105.

Piperno, G., and Z. Ramanis. 1991. The proximal portion of the *Chlamydomonas* flagella contains a distinct set of inner dynein arms. *J. Cell Biol.* 112:701–709.

Piperno, G., Z. Ramanis, E.F. Smith, and W.S. Sale. 1990. Three distinct inner dynein arms in *Chlamydomonas* flagella: molecular composition and location in the axoneme. *J. Cell Biol.* 110:379–389.

Piperno, G., K. Mead, and W. Shestak. 1992. The inner dynein arms I2 interact with a "dynein regulatory complex" in *Chlamydomonas* flagella. *J. Cell Biol.* 118:1455–1464.

Piperno, G., K. Mead, M. LeDizet, and A. Moscatelli. 1994. Mutations in the "dynein regulatory complex" alter the ATP-insensitive binding sites for inner arm dyneins in *Chlamydomonas* axonemes. *J. Cell Biol.* 125:1109–1117.

Porter, M.E. 1996. Axonemal dyneins: assembly, organization, and regulation. *Curr. Opin. Cell Biol.* 8:10–17.

Porter, M.E., J. Power, and S.K. Dutcher. 1992. Extragenic suppressors of paralyzed flagellar mutations in *Chlamydomonas reinhardtii* identify loci that alter the inner dynein arms. *J. Cell Biol.* 118:1163–1176.

Sager, R., and S. Granick. 1953. Nutritional studies with *Chlamydomonas reinhardtii*. *Ann. NY Acad. Sci.* 56:831–838.

Smith, E.F., and W.S. Sale. 1991. Microtubule binding and translocation by inner dynein arm subtype I1. *Cell Motil. Cytoskeleton.* 18:258–268.

Smith, E.F., and W.S. Sale. 1992*a.* Regulation of dynein-driven microtubule sliding by the radial spokes in flagella. *Science (Wash. DC).* 257:1557–1559.

Smith, E.F., and W.S. Sale. 1992*b.* Structural and functional reconstitution of inner dynein arms in *Chlamydomonas* flagellar axonemes. *J. Cell Biol.* 117: 573–581.

Smith, E.F., and W.S. Sale. 1994. Mechanism of flagellar movement and functional interactions between dynein arms and radial spoke/central pair apparatus complex. *In* Microtubules. J.S. Hyams and C.W. Lloyd, editors. Academic Press, New York. 491–496.

Tash, J.S., and G.E. Bracho. 1994. Regulation of sperm motility: emerging evidence for major role of protein phosphatases. *J. Androl.* 15:505–509.

Walzak, C.E., and D.L. Nelson. 1994. Regulation of dynein-driven motility in cilia and flagella. *Cell Motil. Cytoskeleton.* 27:101–107.

Witman, G.B. 1986. Isolation of *Chlamydomonas* flagella and flagellar axonemes. *Methods Enzymol.* 134:280–290.

Witman, G.B. 1992. Axonemal dyneins. *Curr. Opin. Cell Biol.* 4:74–79.